2019

The Isotopic composition of Meteoric Water Along Altitudinal Transects in the Tian Shan of Central Asia

John Bershaw
Portland State University, bershaw@pdx.edu

Alex R. Lechler
Pacific Lutheran University

Citation Details

Bershaw, J., & Lechler, A. (2019). The isotopic composition of meteoric water along altitudinal transects in the Tian Shan of Central Asia. Chemical Geology.

Chemical Geology 516 (2019) 68–78

Contents lists available at ScienceDirect

Chemical Geology

journal homepage: www.elsevier.com/locate/chemgeo

The isotopic composition of meteoric water along altitudinal transects in the Tian Shan of Central Asia

John Bershaw[a,*], Alex R. Lechler[b]

[a] Portland State University, Portland, OR, USA
[b] Pacific Lutheran University, Tacoma, WA, USA

ARTICLE INFO

Editor: Jérôme Gaillardet

Keywords:
Stable isotopes
Meteoric water
Central Asia
Tian Shan
Paleoaltimetry
Paleoclimate
Seasonality
Atmospheric circulation

ABSTRACT

The Tian Shan in Central Asia are a unique mountain range in that they are in the world's most continental location. Seasonal precipitation in the northern Tian Shan is segregated into distinct elevation bands where high elevations receive precipitation primarily during summer and low elevations to the north receive precipitation primarily during the late winter and spring. In this study, we sampled stream water along multiple altitudinal transects to determine the effect unique seasonal patterns of precipitation have on the isotopic composition of surface water. Our results suggest that the northern Tian Shan exhibits an isotopic lapse rate for waters sampled in late spring, but not for those sampled in late summer, when stream water budgets are dominated by high elevation precipitation and snow melt. Deuterium excess results suggest that subcloud evaporation significantly affects the isotopic composition of precipitation at low elevations in spring and that sublimation of snow has a minor impact on $\delta^{18}O$ values of summer melt water. Because high and low elevation $\delta^{18}O$ values are similar, conventional paleoaltimetry based on Rayleigh distillation of an air mass is not applicable to the Kyrgyz Tian Shan. Stream water proxies from the rock record are likely to reflect changes in the seasonal distribution of precipitation which occur on the same spatial scale as altitudinal changes. These results highlight the need to understand modern controls on local stable isotopes of meteoric water in reconstructions of past climate or topography using geologic proxy materials.

1. Introduction

The isotopic composition of meteoric water has been used extensively to characterize the hydrologic cycle worldwide. Stable isotopes ($\delta^{18}O$, $\delta^{2}H$, and increasingly, $\delta^{17}O$) are used to establish groundwater quality (Huang and Pang, 2010) and provenance (Gupta et al., 2005), the relative contribution of glacier melt to surface water (Fan et al., 2015; Karim and Veizer, 2002), and the amount of surface water recycling in arid to semi-arid regions (Bershaw et al., 2012; Li and Garzione, 2017; Wang et al., 2016b). They are also used to distinguish mechanisms of precipitation (Risi et al., 2008; Rohrmann et al., 2014; Rozanski et al., 1993) and constrain the oceanic source of meteoric water (Guan et al., 2013; Tian et al., 2007). Stable isotope geochemistry has also been applied to the rock record using a variety of proxies that constrain environmental change on geologic timescales, including paleoclimate and paleoaltimetry investigations (Bershaw et al., 2010; Garzione et al., 2000; Kar et al., 2016; Kent-Corson et al., 2009; Leier et al., 2013; Mulch et al., 2006; Saylor and Horton, 2014; Wang et al., 2008).

The Tian Shan (Sky Mountains), situated in Central Asia within the countries of Kyrgyzstan, Uzbekistan, Kazakstan, Tajikistan, and China, mark a significant physiographic boundary between Central Asia and the Tarim Basin of west China (Fig. 1). The Tian Shan are the result of crustal thickening forced by Indo-Eurasian plate convergence (Dumitru et al., 2001). However, the temporal-spatial distribution of deformation and associated geodynamic forcing mechanisms throughout the greater Himalayan orogen are not fully understood. Paleoaltimetry, using the isotopic composition of paleo-meteoric water preserved in the rock proxy record, has been applied to both the Himalaya and ranges located deep in the Asian interior, such as the Tian Shan, in an effort to elucidate its geologic evolution (e.g. Caves et al., 2017; Charreau et al., 2012; Graham et al., 2005). Our work aims to clarify modern controls on the isotopic composition of meteoric water across the Tian Shan to better understand how paleoaltimetry can be applied.

Here, we present modern water stable isotope data from three altitudinal transects across the northern Tian Shan in both Kyrgyzstan and China. Our data suggest that subcloud and/or surface evaporation impacts streamwater $\delta^{18}O$ and deuterium excess (d-excess) in this

* Corresponding author.
E-mail address: jbershaw@gmail.com (J. Bershaw).

https://doi.org/10.1016/j.chemgeo.2019.03.032
Received 20 December 2018; Received in revised form 12 February 2019; Accepted 30 March 2019
Available online 01 April 2019

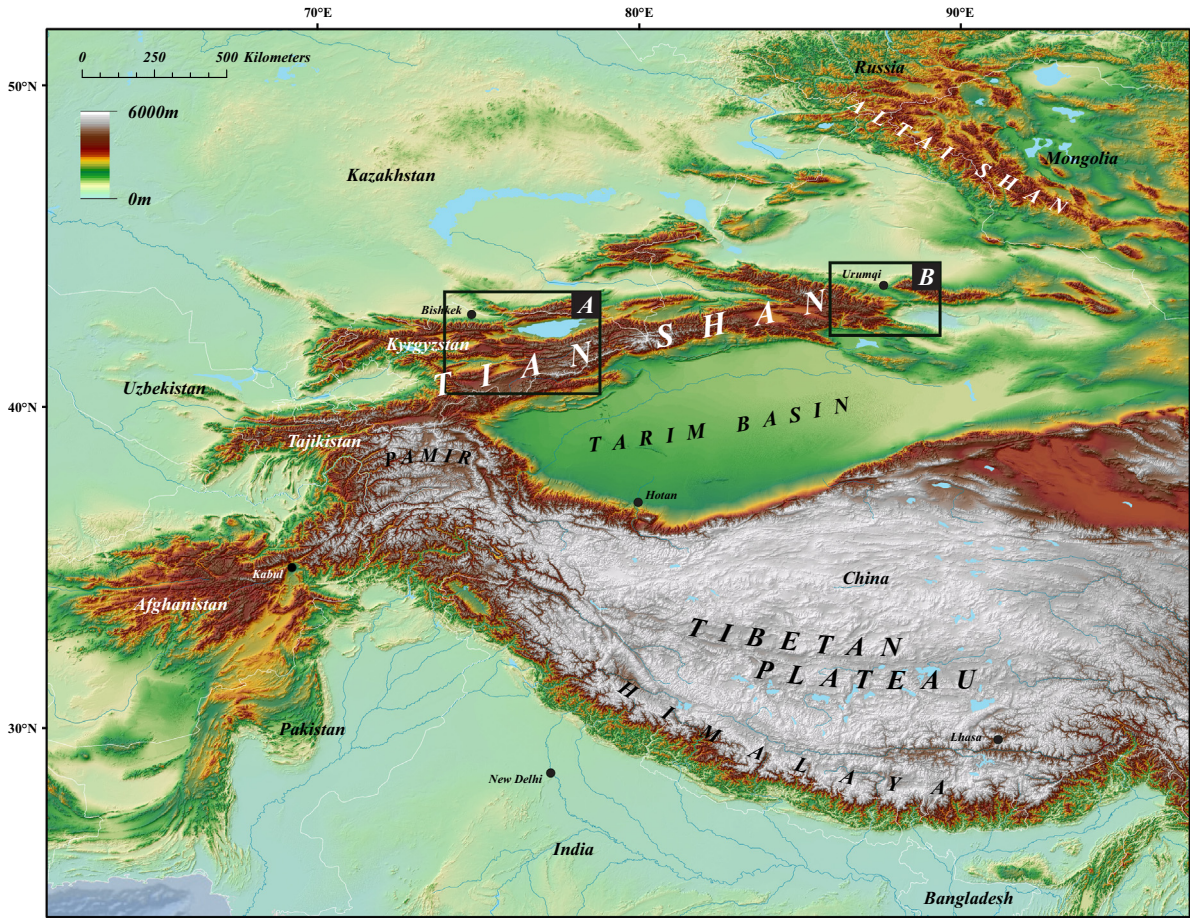

Fig. 1. Location map showing the study area. Detail of study area (A) is shown in Fig. 3A and study area (B) is shown in Fig. 3B. Digital elevation maps (DEM) are from the Shuttle Radar Topography Mission (SRTM).

continental region and that during the summer, high elevation precipitation and sublimation-influenced meltwater dominate the hydrologic budget. This obscures the relationship between the isotopic composition of modern meteoric water and elevation in the Kyrgyz Tian Shan, limiting the accuracy of isotope-based paleoaltimetry. We show unique spatiotemporal patterns in meteoric water $\delta^{18}O$ and d-excess that should be considered when interpreting regional paleoclimate and paleoelevation from water proxies in the rock record.

2. Background

2.1. Climate

Precipitation patterns throughout the Tian Shan are highly variable in both space and time (Böhner, 2006), as revealed through a network of meteorological stations across the region (Wang et al., 2016b) and snow accumulation records at high elevations in the Tian Shan (Aizen et al., 1996). North of the Tian Shan, the majority of precipitation falls during late winter and spring. In contrast, within the Tian Shan and along its southern and eastern flanks, the majority of precipitation falls during the summer (Fig. 2). Flora follow precipitation patterns with summer ombrophiles (plants that flourish in a wet environment) found southeast of the Tian Shan and spring ombrophiles in the Junggar Basin, north of the Tian Shan (Chang, 1983). While low elevation sites like Bishkek, Kyrgyzstan and Urumqi, China on the west and north side of the Tian Shan, respectively, receive considerable precipitation during the spring (Figs. 2 and 3), higher elevations in the foothills and mountains receive the bulk of precipitation during the summer when the subtropical jet shifts to its northern-most position (Fig. 2) (Schiemann et al., 2009). There is also significant spatial variation in annual precipitation amount across the Tian Shan. Precipitation amounts are highest in the mountains (> 400 mm/yr), moderate on the northern flanks (> 200 mm/yr), and minimal on the southern flanks (< 100 mm/yr) (Blumer, 1998). These observations are also reflected in vegetation with prairie in the Chu and Junggar Basins to the north, forests in the mountains, and desert in the Tarim Basin to the south (Klinge et al., 2015). Precipitation amounts in the Tian Shan increase with altitude up to the highest elevations, which contrasts mountains elsewhere that exhibit a limiting elevation above which precipitation amounts do not increase (Barry, 2012). This may be due to the unique seasonal distribution of precipitation in Tian Shan, with high and low elevation moisture derived from unique summer and spring circulations respectively.

This part of central Asia holds the distinction of being located further from an oceanic source than any other location world-wide. As such, moisture travels a long, often complex path from one of many oceanic sources before reaching the Tian Shan (Numaguti, 1999; Tian et al., 2007). During the winter, the Siberian High anti-cyclone develops, resulting in cold, relatively dry conditions throughout most of the Tian Shan (Aizen et al., 1997). The small amount of precipitation that does fall appears to be sourced from the west/southwest, including the Caspian Sea region and Persian Gulf (Bothe et al., 2011). In the spring, the Inter-tropical Convergence Zone (ITCZ) migrates north and mid-latitude westerlies bring moisture from the Atlantic, Mediterranean, and Caspian Sea to the western and northern Tian Shan foothills (Schiemann et al., 2009). During the summer, convective precipitation occurs, but comprises less than half of annual totals, with predominantly cyclonic (advective) activity at higher elevations (Blumer,

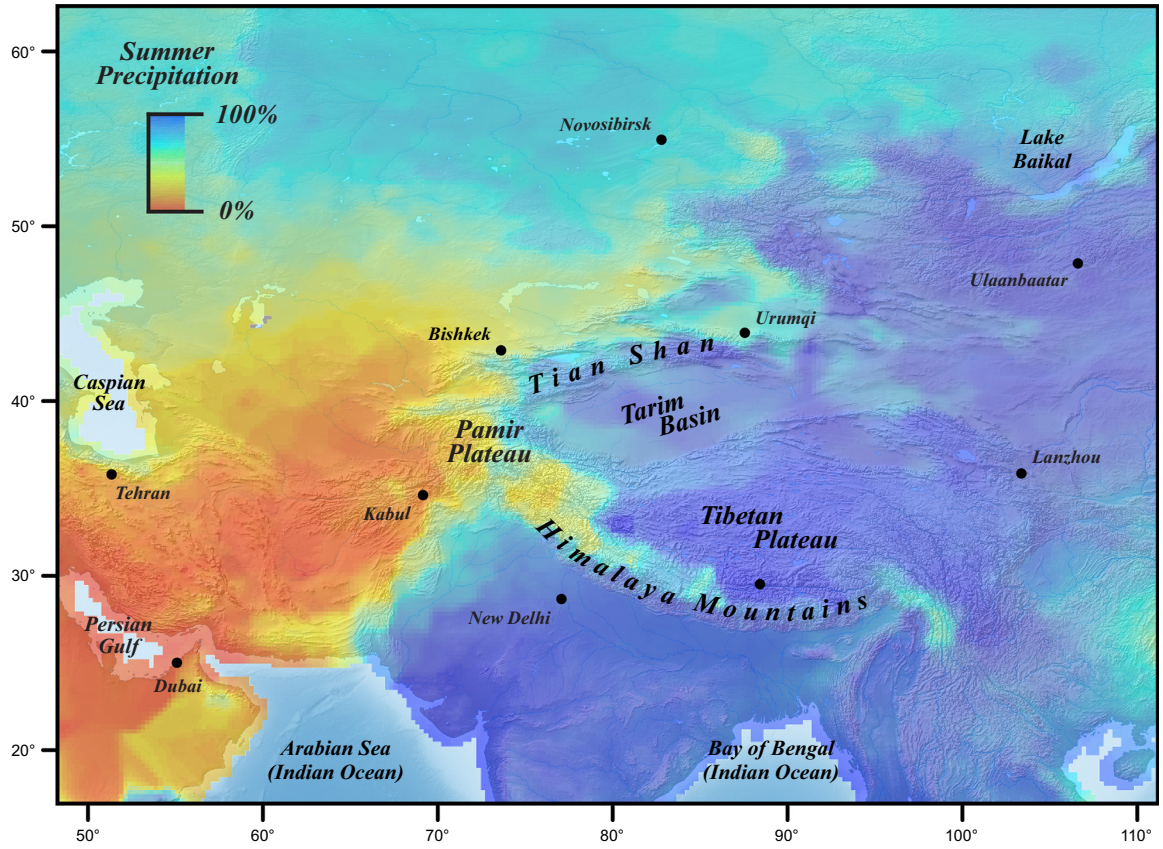

Fig. 2. Map of summer precipitation index, defined as the percentage of summer (May to October) precipitation amount over annual precipitation amount (1980–2010). Regions dominated by summer precipitation will be closer to 100% while regions dominated by winter precipitation will be ~0%. Seasonal precipitation data is from the NOAA Earth System Research Laboratory's GPCC full data reanalysis V6 combined at 1/4° resolution. The basemap is a hillshade raster image from Natural Earth.

1998).

Northwesterlies are a significant source of moisture for summer precipitation in the mountains, with high altitude (> 3000 m) snow accumulating throughout the Tian Shan from May to August (Aizen et al., 1996). In addition, contributions from south and southwesterlies are responsible for extreme precipitation events in the southern Tian Shan and Tarim Basin (Yatagai and Yasunari, 1998; Yu et al., 2003). Climate change over the last few decades has caused an increase in precipitation throughout the region, attributed to enhanced southerlies from an anomalously warm Indian Ocean (Shi et al., 2007). Accordingly, there is a transition from the Tian Shan to the southern Tibetan Plateau of moisture that is ultimately Atlantic-derived to moisture that comes from the Indian and Pacific Oceans (Aizen et al., 1996; Araguás-Araguás et al., 1998; Li and Garzione, 2017; Tian et al., 2001; Yao et al., 2013).

2.2. Isotope systematics

In parts of southeast Asia, seasonal patterns in $\delta^{18}O$ and $\delta^{2}H$ values of precipitation during the Asian monsoon do not correlate with temperature due to the amount effect (Araguás-Araguás et al., 1998). This is because deep convection during the summer (monsoon) lowers $\delta^{18}O$ and $\delta^{2}H$ values of precipitation, due largely to increased Rayleigh distillation of atmospheric water vapor and a more humid air column (Bony et al., 2008; Lee and Fung, 2008; Risi et al., 2008). Conversely, in the Tian Shan and throughout the Tarim Basin, high summer temperatures correlate with relatively high $\delta^{18}O$ and $\delta^{2}H$ values of precipitation. This is more typical of mid-latitudes where relatively high temperatures of vapor formation at the source (oceanic or otherwise) result in less fractionation (higher $\delta^{18}O$ and $\delta^{2}H$ in vapor), the effects of which are observed in precipitation downwind. Increased rates of evapotranspiration during warm summer months also tend to increase the isotopic composition of continental precipitation (Rozanski et al., 1993).

Changes in d-excess, a function of both $\delta^{18}O$ and $\delta^{2}H$, have been interpreted to reflect changes in moisture source throughout Asia (Bershaw et al., 2012; Hren et al., 2009; Karim and Veizer, 2002; Tian et al., 2005). This is because vapor derived from the eastern Mediterranean Sea has uniquely high d-excess values (~20‰) relative to the global average (~10‰) (Gat and Carmi, 1970), as defined by the y-intercept of the Global Meteoric Water Line (GMWL) (Craig, 1961):

$$\delta^{2}H = 8 * \delta^{18}O + 10 \quad (1)$$

Accordingly, higher d-excess values for Asian meteoric waters have often been associated with westerly derived precipitation and lower values associated with southerly or monsoonal moisture (Tian et al., 2007).

It has also been shown that d-excess values of vapor and precipitation can vary significantly based on local environmental conditions, such as the temperature of condensation, amount of subcloud evaporation during rainout, and degree of local moisture recycling (Cui et al., 2009; Froehlich et al., 2008; Gat and Airey, 2006; Jouzel and Merlivat, 1984; Kurita and Yamada, 2008; Liotta et al., 2006; Rank and Papesch, 2005; Wang et al., 2016a). A direct relationship between d-excess and elevation is observed in the Himalaya and on the windward side of mountains generally, where high elevations are associated with relatively high d-excess values of surface water (Bershaw, 2018; Froehlich et al., 2008; Kong et al., 2013). This may be due to more significant amounts of subcloud evaporation at lower elevations as raindrops fall through a relatively tall and warm air column, decreasing

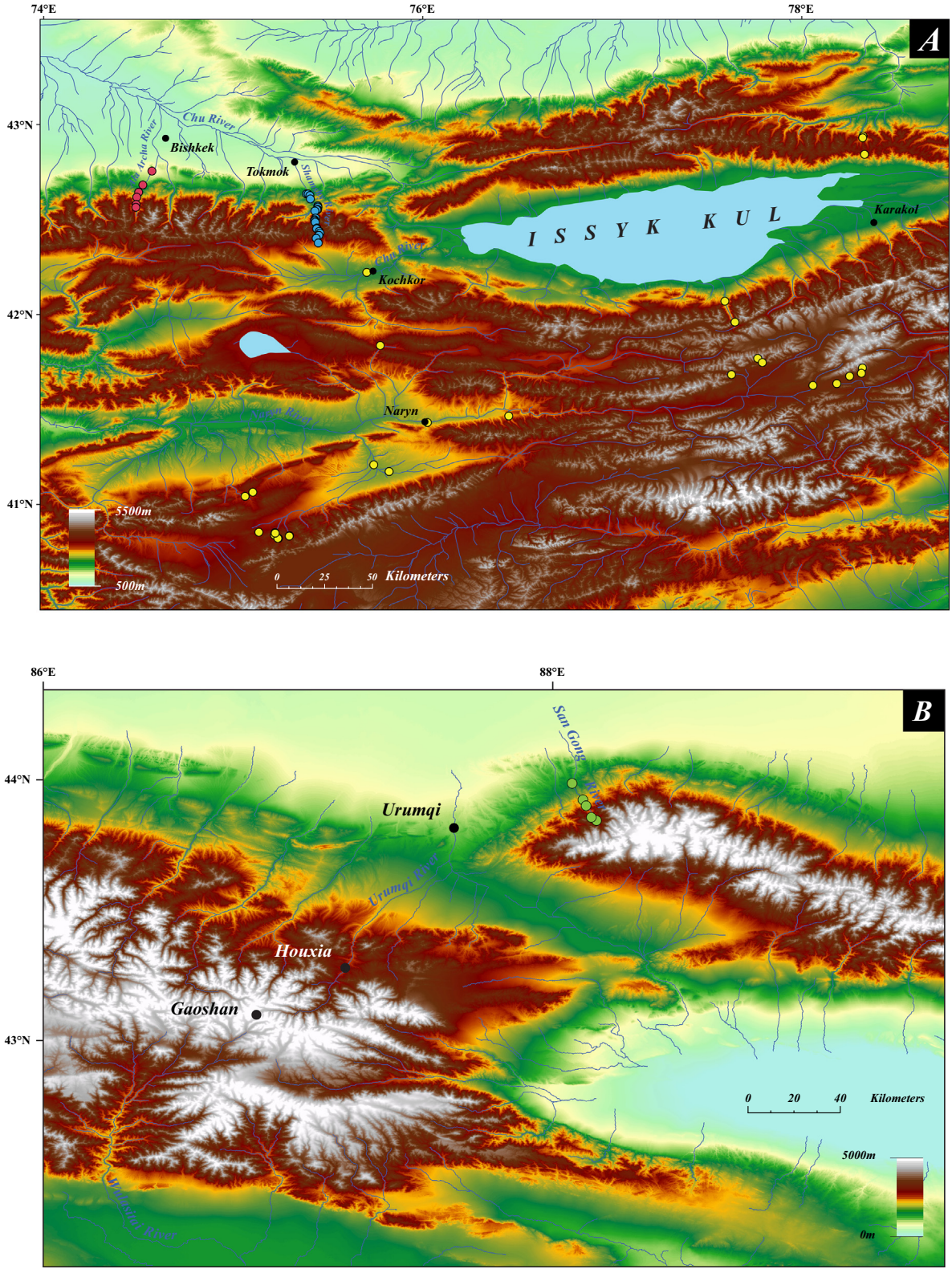

Fig. 3. (A) High resolution DEM showing transects along the northern flank of the Kyrgyz Tian Shan near Bishkek, Kyrgyzstan. Red and blue circles correspond with sample locations on the Ala Archa (sampled in spring) and Shamshy Rivers (sampled in late summer) respectively. Yellow circles show locations of published stream samples from Issyk Kul Basin (sampled in late summer/early fall) (Macaulay et al., 2016). Map is shown as rectangle A in Fig. 1. (B) High resolution DEM of the northern flank of the Chinese Tian Shan near Urumqi, China. Green circles correspond to sample locations along the San Gong River sampled in spring. Map is shown as rectangle B in Fig. 1. (For interpretation of the references to color in this figure legend, the reader is referred to the web version of this article.)

d-excess values of precipitation at low elevations.

2.3. Paleoaltimetry

A definable inverse relationship between elevation and the isotopic composition of meteoric water ($\delta^{18}O$ and $\delta^{2}H$) exists on the windward side of mountains (altitude effect), conforming to a Rayleigh distillation model of air mass depletion (Rowley and Garzione, 2007). Modern isotope-elevation relationships (isotopic 'lapse rates') globally average −2.8/km elevation gain (Poage and Chamberlain, 2001). This modern relationship has been used to constrain temporal changes in a region's paleoelevation (paleoaltimetry) through the isotopic composition of ancient water, inferred from proxies in the rock record such as paleosol and lacustrine carbonates, mammal teeth, volcanic glass, lipid biomarkers, and select clays (Cerling and Quade, 1993; Friedman et al., 1993; Kohn and Cerling, 2002; Rowley and Garzione, 2007; Sachse et al., 2012; Savin and Hsieh, 1998). Each paleoaltimeter may reflect different types of meteoric water and integrate over unique time scales (Rowley and Garzione, 2007). For example, paleosol carbonates likely reflect rainfall that infiltrates the soil during the season of carbonate precipitation (Breecker et al., 2009; Cerling and Quade, 1993). Fluvial carbonate cements, lacustrine carbonates, and palustrine (flood plain) paleosol carbonates are more likely to precipitate from surface and groundwater, sourced from precipitation that falls within the watershed throughout the year (Talbot, 1990). In both cases, individual carbonate samples are thought to integrate water over thousands to tens of thousands of years (Gile et al., 1966).

In straightforward applications of the altitude effect, it is often presumed that as a mountain range grows, the $\delta^{18}O$ and $\delta^{2}H$ values of meteoric water and associated rock proxies decrease in response. However, this relationship may be complicated by subcloud and surface water evaporation and/or recycling, common in arid environments (Gat, 1996). These processes may obscure the relationship between the isotopic composition of meteoric water and elevation (Bershaw et al., 2016; Kurita and Yamada, 2008), limiting the accuracy of isotope-based paleoaltimetry. This highlights the need to understand modern controls on local stable isotopes of meteoric water in reconstructions of past climate or topography using geologic proxy materials.

3. Methods

Our strategy was to collect stream water in the northern Tian Shan to constrain isotopic lapse rates along the windward side of the range (Fig. 1) to evaluate whether conventional stable isotope paleoaltimetry principles (e.g. Chamberlain and Poage, 2000) are applicable to this continental location. We followed the approach of Garzione et al. (2000) by sampling small catchments ($< 100\,km^2$) when possible in order to minimize the elevation range and catchment area represented by each water sample. Because we are interested in using results to better inform the interpretation of paleowater proxies, we targeted stream waters as these have been shown to integrate numerous precipitation events, similar to what is observed in seasonally averaged precipitation records (Kendall and Coplen, 2001). In total, 32 stream water samples were collected. Annual precipitation totals for the years of sample collection (2008 and 2009) in nearby Bishkek, Kyrgyzstan (331 mm and 406 mm, respectively) were similar to the yearly average from 1901 to 2015 (376 mm; World Bank, 2018) suggesting meteoric water samples analyzed here are representative of the long-term local climate. Soil water was not collected because of the relative difficulty in doing so. All samples were collected and sealed in plastic test tubes using teflon tape and external electrical tape. Samples were stored in refrigeration prior to isotopic analysis ($\delta^{18}O$ and $\delta^{2}H$).

Due to timing of sample collection and instrumentation availability, samples were analyzed in two different labs, using either mass spectrometry (MS) or laser absorption spectroscopy (LAS). Analyses completed at the University of Rochester in 2008 were done via MS. For oxygen analyses, ~0.5 mL of each water sample was loaded into a 12 mL Exetainer™ and flushed with a mixture of 0.3% CO_2 and UHP helium. Tubes were allowed to equilibrate for at least 18 h at ambient room temperature prior to analysis. Headspace CO_2 gas was then drawn into a Thermo Delta plus XP mass spectrometer in continuous-flow mode via a Thermo Gas Bench peripheral and a GC-PAL autosampler for analysis. $\delta^{18}O$ results are calculated using internal laboratory standards calibrated to Vienna Standard Mean Ocean Water (VSMOW) and Standard Light Antarctic Precipitation (SLAP) with 1σ uncertainties of ± 0.10‰. Hydrogen analyses were run in continuous-flow mode via a Thermo Electron TC/EA peripheral. Approximately 200 nL of sample water was injected into the TC/EA during three successive injections. The reactor was set at a temperature of 1450 °C and the GC oven was set at 90 °C. The average of four injections indicates a 1σ uncertainty better than ± 2.0‰.

Analyses completed at the University of Rochester in 2010 were made by LAS on a Los Gatos Research Liquid Water Isotope Analyzer (LWIA-24d DLT-100) with a GC-PAL autosampler. Approximately 900 nL of water was injected into a heated, evacuated block. Water was vaporized and drawn into a laser cavity, where absorption analysis took place. Reported results are the average and standard deviation of 5–10 adjacent injections and measurements of a water sample from a single vial. Standardization is based on internal standards referenced to VSMOW and Standard Light Antarctic Precipitation (VSLAP). The 1σ uncertainties of H and O isotopic results are ± 1.2‰ and ± 0.1‰ respectively, unless otherwise indicated.

Analyses completed at the University of Arizona in 2009 were made using a dual inlet MS (Delta-S, Thermo Finnegan, Bremen, Germany) equipped with an automated chromium reduction device (H-Device, Thermo Finnegan) for the generation of H gas using metallic chromium at 750 °C. Water $\delta^{18}O$ was measured on the same mass spectrometer using an automated CO_2-H_2O equilibration unit. Standardization is also based on internal standards referenced to VSMOW and VSLAP. The 1σ uncertainties of H and O isotopic results from this lab are better than ± 1‰ and ± 0.08‰ respectively.

4. Results

We present stream water $\delta^{18}O$, $\delta^{2}H$, and d-excess values for three different altitudinal transects on the northern flank of the Tian Shan (Table 1). The first was collected near Bishkek, Kyrgyzstan up the Ala Archa River valley in April of 2008 with a sample site elevation range from 1100 to 2106 m (Fig. 3A). The second was collected near Urumqi, China up the San Gong River in May of 2008 with an elevation range from 980 to 1918 m (Fig. 3B). The last was collected near Bishkek up the Shamshy River valley in August of 2009 with an elevation range from 1391 to 3387 m (Fig. 3A). Because these are stream water samples, the mean elevations of contributing watersheds are used in elevation plots. Mean basin hypsometries (MBH) were estimated using the ArcGIS Spatial Analyst Hydrology Toolbox. Watershed size among individual transects varies considerably where trunk streams are more prevalent in Ala Archa and San Gong transects (average area ~181 km^2) and smaller tributaries dominate the Shamshy transect (average area ~32 km^2) (Table 1).

The $\delta^{18}O$ values of all stream water samples average −10.3‰, generally consistent with global precipitation during the summer at these latitudes (42–44°N) (Rozanski et al., 1993). Stream water $\delta^{18}O$ values are also similar to relatively low elevation (~800 m) spring and fall precipitation at Bishkek, Kyrgyzstan and Urumqi, China (Fig. 4), in addition to annual precipitation throughout the Tian Shan which averages −9.1‰ (Wang et al., 2016b). Results from surface water samples collected during different seasons and over a range of elevations were relatively invariant with a range in $\delta^{18}O$ of 3.3‰ and standard deviation of 0.76‰. Deuterium excess (d-excess) values range from 9.9 to 19.8‰ with an average of 15.1‰, higher than the global average (10‰), but consistent with high elevation precipitation on the

Table 1
Isotope and meta-data for samples collected in this study. The location of each transect is shown in Fig. 3. We calculated mean basin hypsometry (MBH) and watershed centroids for each sample.

Sample	$\delta^{18}O$ (‰)	δD (‰)	d excess (‰)	Elevation (m)	MBH (m)	Basin_area (km^2)	Latitude	Longitude	Latitude (centroid)	Longitude (centroid)	Transect	Date collected
JBTS-64	−10.5	−72.4	11.8	1471	3040	155.0	43.9140	88.1860	43.8381	88.1849	San Gong	5/10/2008
JBTS-62	−8.6	−58.4	10.2	1856	2562	3.0	43.8725	88.1220	43.8597	88.1962	San Gong	5/10/2008
JBTS-60	−10.9	−74.1	12.7	1918	3349	103.7	43.8565	88.2062	43.8173	88.2052	San Gong	5/10/2008
JBTS-57	−9.8	−64.7	13.3	1382	2851	190.0	43.9358	88.1770	43.8538	88.1759	San Gong	5/9/2008
JBTS-56	−10.9	−70.5	16.8	980	2695	214.1	44.0016	88.0605	43.8659	88.1641	San Gong	5/9/2008
JBTS-40	−10.0	−66.9	12.9	1100	2990	320.2	42.7544	74.5633	42.5641	74.4966	Ala Archa	4/29/2008
JBTS-39	−11.4	−73.9	17.5	2106	3564	102.8	42.5629	74.4788	42.4841	74.4848	Ala Archa	4/29/2008
JBTS-38	−11.2	−72.8	16.9	1979	3528	181.8	42.5784	74.4806	42.5099	74.4841	Ala Archa	4/29/2008
JBTS-37	−10.9	−71.8	15.4	1502	3429	204.7	42.6167	74.4833	42.5193	74.4844	Ala Archa	4/29/2008
JBTS-36	−10.8	−72.7	13.7	1503	3319	235.3	42.6421	74.4934	42.5319	74.4815	Ala Archa	4/29/2008
JBTS-35	−10.9	−70.4	17.1	1359	3175	276.0	42.6810	74.5155	42.5465	74.4871	Ala Archa	4/29/2008
JBTS-128	−9.7	−64.0	13.8	2576	3182	21.1	42.3744	75.4433	42.4069	75.4420	Shamshy	8/28/2009
JBTS-126	−9.3	−63.2	11.2	2739	3229	6.9	42.3989	75.4327	42.4197	75.4298	Shamshy	8/28/2009
JBTS-125	−9.5	−62.1	13.5	3097	3526	2.2	42.4145	75.4467	42.4266	75.4552	Shamshy	8/28/2009
JBTS-124	−8.7	−54.6	15.1	3097	3481	0.5	42.4145	75.4467	42.4172	75.4543	Shamshy	8/28/2009
JBTS-123	−10.6	−68.7	15.8	3387	3645	0.9	42.4269	75.4527	42.4301	75.4618	Shamshy	8/28/2009
JBTS-121	−9.4	−58.4	16.5	3387	3497	0.3	42.4354	75.4485	42.4342	75.4530	Shamshy	8/28/2009
JBTS-120	−10.5	−67.7	16.4	2935	3340	4.0	42.4494	75.4347	42.4387	75.4423	Shamshy	8/27/2009
JBTS-119	−11.3	−71.1	19.6	2880	3553	13.1	42.4533	75.4364	42.4494	75.4766	Shamshy	8/27/2009
JBTS-118	−10.5	−66.1	18.2	2729	3308	1.3	42.4841	75.4273	42.4743	75.4156	Shamshy	8/27/2009
JBTS-117	−10.1	−65.3	15.7	2704	3032	1.0	42.4906	75.4243	42.4889	75.4157	Shamshy	8/27/2009
JBTS-116	−10.0	−63.7	16.3	2635	3002	0.3	42.4971	75.4240	42.4965	75.4178	Shamshy	8/27/2009
JBTS-115	−9.6	−58.9	17.9	2545	3467	2.6	42.5060	75.4294	42.4931	75.4461	Shamshy	8/26/2009
JBTS-114	−10.6	−65.7	19.2	1918	3267	69.3	42.5429	75.4257	42.4708	75.4419	Shamshy	8/26/2009
JBTS-113	−10.3	−62.6	19.8	1971	2232	1.1	42.5501	75.4362	42.5411	75.4420	Shamshy	8/26/2009
JBTS-112	−10.6	−65.4	19.4	1982	3181	22.9	42.5509	75.4406	42.5139	75.4703	Shamshy	8/26/2009
JBTS-111	−10.2	−66.0	15.7	1818	2751	18.3	42.5637	75.4417	42.5446	75.4816	Shamshy	8/26/2009
JBTS-110	−10.1	−69.0	11.5	1817	2179	3.6	42.5704	75.4414	42.5753	75.4588	Shamshy	8/26/2009
JBTS-108	−9.7	−63.8	13.4	1391	2515	36.2	42.6071	75.4018	42.5834	75.3344	Shamshy	8/25/2009
JBTS-107	−11.0	−76.0	12.2	1391	1890	1.0	42.6252	75.3992	42.6225	75.4130	Shamshy	8/25/2009
JBTS-106	−10.1	−66.6	14.3	1392	2932	462.6	42.6331	75.3900	42.5086	75.3467	Shamshy	8/24/2009
JBTS-105	−11.9	−85.2	9.9	1438	1768	2.3	42.6339	75.3811	42.6248	75.3716	Shamshy	8/24/2009

windward side of ranges elsewhere (e.g. Froehlich et al., 2008; Gonfiantini et al., 2001; Tian et al., 2005).

Of the three elevation transects, two exhibit local meteoric water lines (LMWL) with slopes significantly lower than the global average of 8. These are Ala Archa (m = 4.7, R^2 = 0.86) and the San Gong (m = 6.3, R^2 = 0.92) (Fig. 5). Both were sampled in the spring (April and May, respectively). The third transect, up the Shamshy River, shows an LMWL close to the GMWL (m = 7.7, R^2 = 0.80). This transect was sampled in August.

Isotopic lapse rates are observed for both the Ala Archa transect (−2.5‰/km, R^2 = 0.82) and San Gong transect (−5‰/km, R^2 = 0.40), but the significance of these is questionable as they span short ranges of MBH (574 m and 787 m respectively) and are based on few data points (Fig. 6). The Shamshy transect, sampled in August and covering a larger range of elevations (1877 m) with more samples (n = 21), does not show a significant relationship between $\delta^{18}O$ and MBH (R^2 = 0.18) (Fig. 7A). This is also the case when only windward samples (solid circles) are considered (R^2 = 0.08). This is consistent with published stream water results from other parts of the Tian Shan and Pamir that receive precipitation predominantly during summer months, including the intermontane Issyk Kul Basin (Fig. 7B) (Macaulay et al., 2016) and interior (east side) of the Pamir Plateau (open circles in Fig. 7C) (Liu et al., 2014), all sampled in late summer and early fall.

5. Discussion

5.1. Local meteoric water lines

The difference in local meteoric water lines (LMWL) for transects of this study (Fig. 5) may be related to when (seasonally) streams were sampled. Relatively low slopes (m < 6.4) indicative of evaporative enrichment (Craig, 1961) characterize the Ala Archa and San Gong transects sampled in the late spring (April–May). It is possible that precipitation contributing to surface runoff in these catchments is modified by subcloud and/or surface evaporation, consistent with trends observed in precipitation elsewhere in the Tian Shan (Wang et al., 2016a) and on the windward side of mountains generally (Bershaw, 2018; Froehlich et al., 2008; Kong et al., 2013; Liotta et al., 2006). The Shamshy transect does not show a significant evaporative LMWL (m = 7.7), but is unique in that it was sampled in late summer (August). This is consistent with summer stream water from the Pamir in Tajikistan (Liu et al., 2014). The lack of a significant evaporative signal in late summer may be due to a water budget during summer months dominated by relatively high elevation precipitation (> 2000 m) which is less affected by subcloud evaporation. While it is difficult to know a priori the time period of integration for sampled stream waters and whether the timing of stream sampling impacted the observed isotopic trends, the variability in LMWL among transects suggests seasonal climate is affecting stream water $\delta^{18}O$ in the Tian Shan. Such seasonality of stream water $\delta^{18}O$ has been documented in rivers worldwide (Kendall and Coplen, 2001; Lu et al., 2012).

We consider whether differences in LMWL for sample transects reflect variation in catchment size as San Gong and Ala Archa transects generally integrate wider swaths of space and time than those from Shamshy (Table 1). Because larger catchments are associated with longer residence times of surface and groundwater, the likelihood of exposure and evaporative enrichment in these catchments may be higher. However, if this were the case, more evaporation in large basins should affect d-excess values (lower d-excess in basins with a larger area) which is not observed in our dataset (R^2 = 0.00), suggesting that differences in LMWL for sample transects are not related to catchment size.

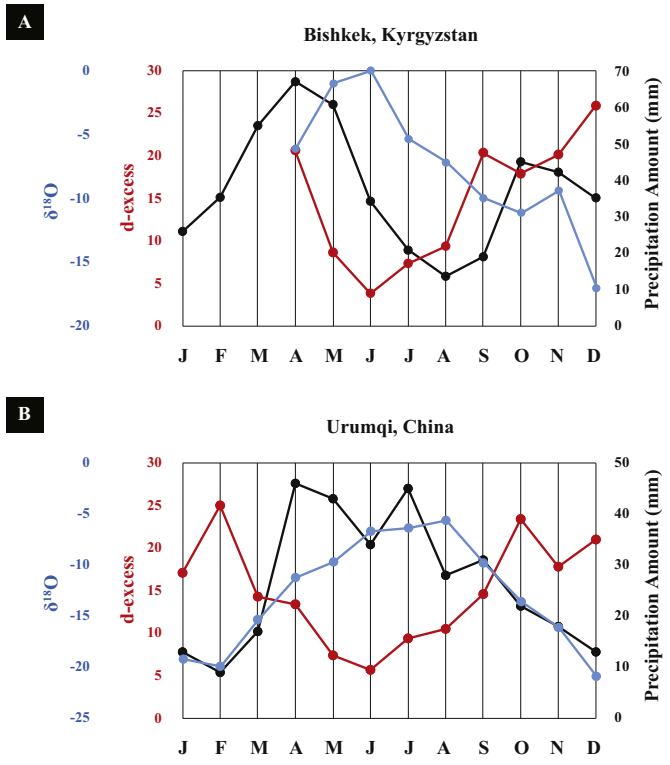

Fig. 4. (A) Monthly average precipitation amount (black) and isotopic composition (blue is $\delta^{18}O$ and red is d-excess) of precipitation samples taken at Bishkek, Kyrgyzstan from 2001 to 2002. Isotope data is from Morris et al. (2005) and was filtered by d-excess > 0‰ to remove rain significantly affected by subcloud evaporation. Isotope data was not reported for Jan-Mar. Monthly precipitation amount data spans 1961–1990 and is from the National Oceanic and Atmospheric Administration (NOAA) Global Climate Observing System (GCOS). (B) Same symbology as (A), but for Urumqi, China over 11 years from 1986 to 2003. Data is from GNIP (IAEA/WMO, 2018). Though the seasonal distribution of precipitation differs between sites, both show a similar difference between winter and summer $\delta^{18}O$ (> 15‰). (For interpretation of the references to color in this figure legend, the reader is referred to the web version of this article.)

5.2. Seasonal variation in isotopic composition

The seasonal (Jun to Dec) ranges in $\delta^{18}O$ and d-excess of modern precipitation at Urumqi, China and Bishkek, Kyrgyzstan are significant, reaching 15‰ and 20‰ respectively (Fig. 4). Seasonal variation is due to changes in temperature and relative humidity at the moisture source and evaporation over the continent (affecting the y-intercept and slope of Eq. (1)) (Rozanski et al., 1993). In contrast, our samples were collected at different times of the year but do not show seasonal variability in $\delta^{18}O$ or d-excess. The Shamshy transect sampled in late summer has $\delta^{18}O$ values that average −10‰ (range of 3.2‰) (Table 1). This is consistent with a mix of summer rainfall for Tian Shan sites > 1 km in elevation which average −6.4‰ (Wang et al., 2016b), and snow/ice on Inylchek glacier which averages ~−15‰ (Aizen et al., 1996; Kreutz et al., 2003). The average $\delta^{18}O$ value along the Shamshy transect is almost identical to glacier meltwater during summer in the Issyk Kul Basin, which averages −10.8‰ (Macaulay et al., 2016), suggesting that streams are largely fed by high elevation meltwater in late summer.

The Ala Archa and San Gong transects, each sampled in spring, have $\delta^{18}O$ values that average −11‰ (range of 1.0‰) and −10‰ (range of 2.3‰) respectively, similar to the Shamshy transect sampled in late summer. Like Shamshy, the average $\delta^{18}O$ values of streams sampled in spring (Ala Archa and San Gong) are consistent with high elevation meltwater. However, their evaporative LMWLs (low slopes) suggest low elevation evaporation is significant. This could be explained by the integration of low elevation precipitation experiencing subcloud evaporation, as the average isotopic composition of water sampled is also consistent with spring precipitation in Bishkek, Kyrgystan and Urumqi, China (Fig. 4).

Average d-excess values are also similar among transects with Ala Archa and San Gong transects averaging 16‰ (range of 5.0‰) and 13‰ (range of 6.6‰) respectively, while the Shamshy transect sampled in late summer has an average d-excess value of 16‰ (range of 9.9‰). As is the case with $\delta^{18}O$ values, d-excess values could be explained by either late spring precipitation at Bishkek and Urumqi (Fig. 4) or a combination of high elevation rainfall, which averages 8‰ (Wang et al., 2016b), and meltwater derived from high elevation snow/ice which averages 23‰ (Kreutz et al., 2003). By simply comparing average $\delta^{18}O$ and d-excess values, the Shamshy watershed sampled in late summer, which is presumed to be dominated by high elevation snow melt, is isotopically similar to watersheds sampled in spring (Ala Archa and San Gong), where stream water is more likely derived from a combination of meltwater and local spring precipitation. Thus, stream water in the Tian Shan is not easily distinguished based on isotopic

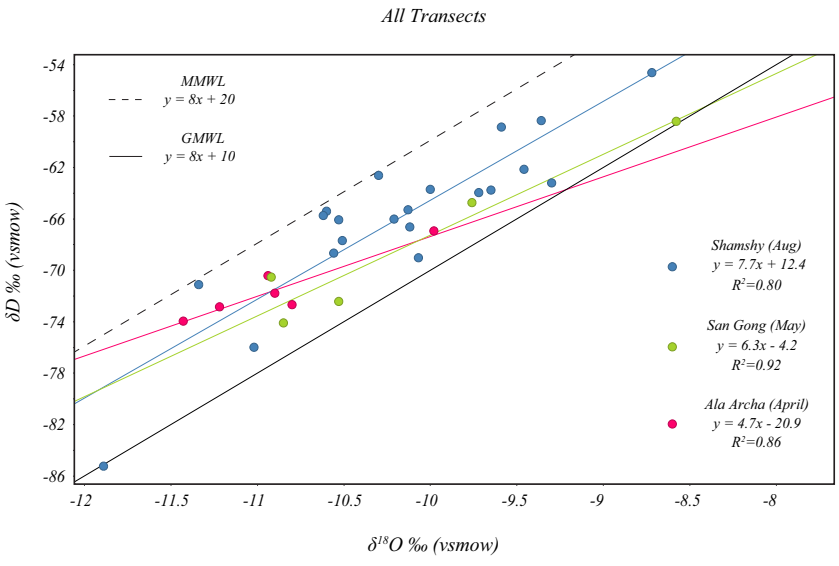

Fig. 5. Local Meteoric Water Lines (LMWL) for all three transects. Color-coded by transect, consistent with coloring used in location maps (Fig. 3). The GMWL and Mediterranean Meteoric Water Line (MMWL) are shown for reference. Transects sampled in spring have slopes much < 8 suggesting evaporation is significant. This may be due to subcould evaporation at relatively low elevations. Late summer river water (Shamshy transect) appears to be dominated by high elevation precipitation and snow melt at all elevations. Analytical uncertainties are < ± 2‰ for δD and < ± 0.1‰ for $\delta^{18}O$. (For interpretation of the references to color in this figure legend, the reader is referred to the web version of this article.)

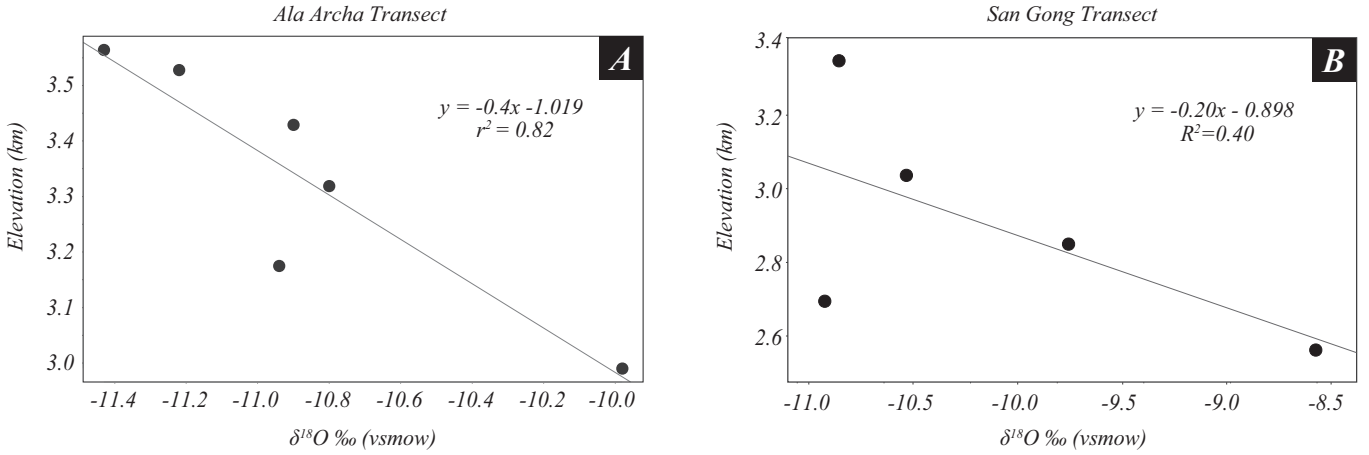

Fig. 6. Isotopic lapse rates for transects in the Tian Shan. Elevation in all plots is reported as the mean basin hypsometry. (A) The Ala Archa transect in Kyrgyzstan (location in Fig. 3A), sampled in spring, is characterized by an isotopic lapse rate of 0.4 km/−1‰ (or −2.5‰/km elevation gain), consistent with the global average (Poage and Chamberlain, 2001). (B) The San Gong transect in China (location in Fig. 3B), also sampled in spring, is characterized by an isotopic lapse rate of 0.2 km/−1‰ (or −5‰/km elevation gain). The limited range of elevations represented makes interpretation of an isotopic lapse rate uncertain.

composition alone.

5.3. Isotopic lapse rates

The lack of a $\delta^{18}O$ - elevation relationship along the Shamshy transect in summer (Fig. 7A) is consistent with a seasonal precipitation regime partitioned by elevation (Fig. 2). Our data suggests that in the Tian Shan during summer and early fall, the water budget is dominated by high elevation precipitation and snow melt, which results in a flat or non-existent isotopic lapse rate. Elsewhere, the absence or reduction of isotopic lapse rates are often attributed to conditions in the rainshadow (e.g. Lechler and Niemi, 2011a). This explanation likely does not apply to the northern flanks of the central Tian Shan as most precipitation is thought to be sourced from westerlies (Aizen et al., 1996; Liu et al., 2015), putting these transects sampled on the windward side of the range (as opposed to lee or rainshadow). Snow sublimation at high elevations may contribute to a late summer decrease in the isotopic lapse rate as seen in the semi-arid southwestern United States (Lechler and Niemi, 2011b). Sublimation of snow can lead to an increase in surface water $\delta^{18}O$ values at high elevations, decreasing the magnitude of $\delta^{18}O$-elevation gradients. This contrasts Kreutz et al. (2003) who argue that sublimation at high elevations in the Tian Shan is minor due to a LMWL that is not indicative of evaporation (m = 6.9, their data), and reasoning that low temperatures during winter (dry season) and high snow accumulation rates during summer limit sublimation. Although the evaporation of high elevation water and snow sublimation may explain higher $\delta^{18}O$ values of some samples (Fig. 7A), a non-evaporative LMWL along the Shamshy transect (m = 7.7) (Fig. 5) supports the interpretation of Kreutz et al. (2003) of limited sublimation influence and suggests that the lack of an isotopic lapse rate across the ~2 km elevation span of the Shamshy transect is the result of a watershed dominated by precipitation and snowmelt originating at high elevations (> 3 km) in the catchment.

The lack of an isotopic lapse rate along the Shamshy transect is also consistent with stream water data from the inter-montane Issyk Kul Basin sampled in summer and early fall by Macaulay et al. (2016). When Issyk Kul sample locations are adjusted to mean basin elevations (mean basin hypsometry or MBH), an isotopic lapse rate is not observed (Fig. 7B). Lack of a significant isotopic lapse rate is also observed in surface water from the east Pamir where summer precipitation dominates (open circles in Fig. 7C) (Liu et al., 2014) and the intermontane Kaidu River Basin ~200 km southwest of Urumqi, China (Haiyan et al., 2018). This is also the case for stations sampling precipitation throughout the Tian Shan (Aizen et al., 1996; Wang et al., 2016b). Specifically, annual weighted precipitation $\delta^{18}O$ values at Tian Shan sites that are > 1 km in elevation are, on average, ~3‰ higher than those at sites < 1 km in elevation (Wang et al., 2016b). Wang et al. (2016b) show that air temperature is an important control on precipitation isotopes and suggest that the lack of an altitude effect is related to the seasonal distribution of precipitation across the range. The observation that surface water is relatively enriched at high elevations along the Shamshy transect and others, with $\delta^{18}O$ values > −10‰ above 3 km elevation (Fig. 7A), indicates that a model of Rayleigh distillation does not accurately characterize the isotopic composition of summer stream water on the northern, windward side of the Kyrgyz Tian Shan. Our interpretation that this is because watersheds are dominated by high elevation snow melt and precipitation is consistent with interpretations by Liu et al. (2014) for the Pamir in Tajikistan.

Though isotopic lapse rates are observed during spring for both the Ala Archa transect (−2.5‰/km, R^2 = 0.82) and San Gong transect (−5‰/km, R^2 = 0.40), the limited elevation range (574 m and 787 m respectively) and limited number of data points makes the relationship speculative (Fig. 6). We test their reliability as related to small sample populations (n ≤ 6) by randomly sampling the Shamshy dataset, where there is no observed correlation between $\delta^{18}O$ and elevation (R^2 = 0.18) to see if we generate false positives. We start by selecting 1000 random Shamshy samples from the 2.5–3.6 km elevation range (n = 16) because that overlaps the elevations in Ala Archa and San Gong transects. We bin these into groups of five (200 groups total) to correspond with the number of samples collected along each transect (n ≤ 6). A correlation coefficient (R^2 value) is calculated between $\delta^{18}O$ and elevation for each group of five random samples. The average R^2 of these 200 correlations is 0.30, less than that observed along both Ala Archa and San Gong transects. Though sample populations are small, this suggests isotopic lapse rates in spring do exist along these transects. Evaporation of low elevation water, evidenced by low LMWL slopes (Fig. 5), may enhance isotopic lapse rates. An isotopic lapse rate on the northernmost flank of the Kyrgyz Tian Shan during spring is also consistent with one observed in the western Pamir in Tajikistan for sites dominated by winter/spring precipitation (solid circles in Fig. 7C) (Liu et al., 2014).

It is also possible that differences in watershed size between these transects sampled in spring (average area ~181 km^2) and the Shamshy transect sampled in late summer (average area ~32 km^2) is affecting the observed discrepancy in $\delta^{18}O$ - elevation correlation. Regardless, we believe the lack of isotopic lapse rate observed in the Shamshy dataset is robust, as it is based on a relatively large number of samples and is consistent with other stream water datasets throughout the region.

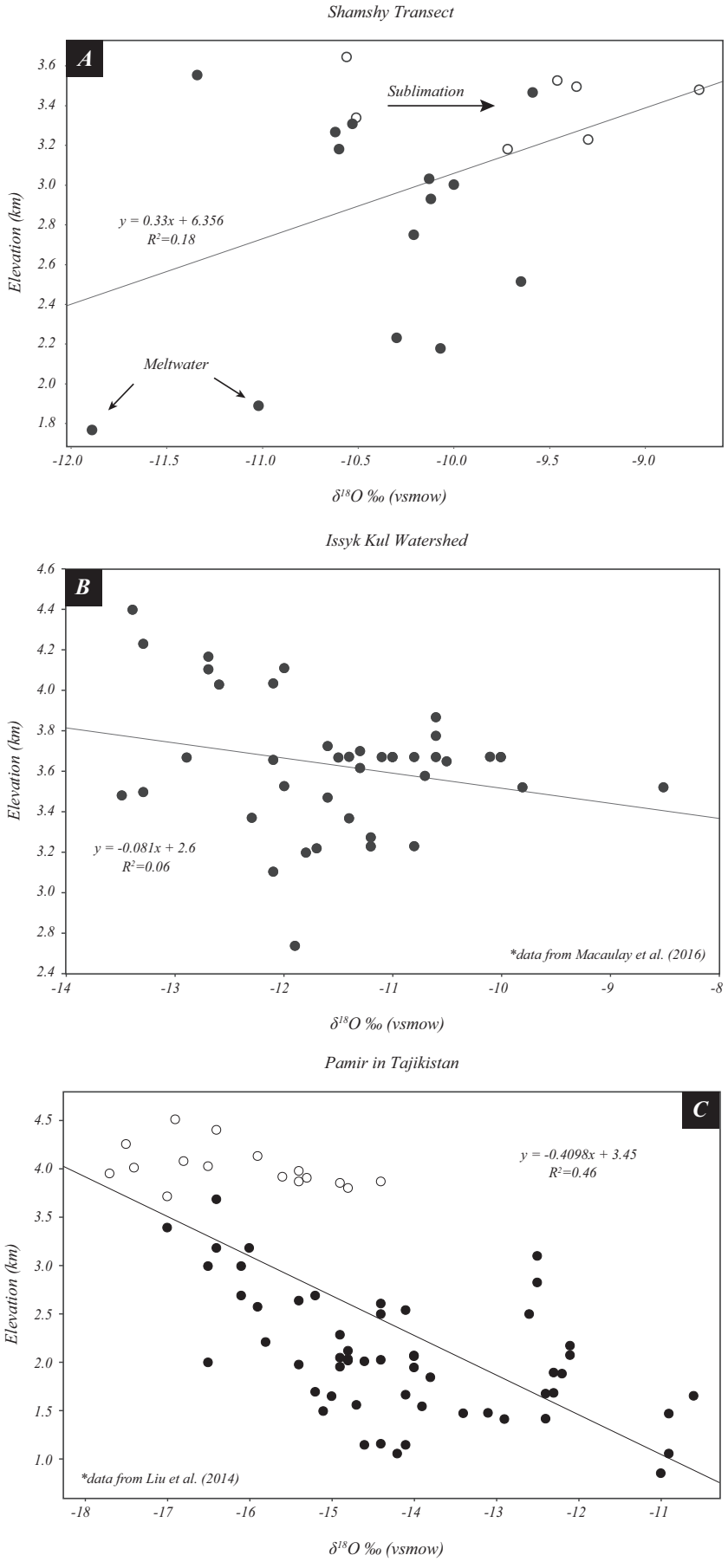

Fig. 7. (A) The Shamshy transect in Kyrgyzstan, sampled in late summer (location in Fig. 3A), does not show a significant relationship between $\delta^{18}O$ and elevation. We suggest that the lack of an apparent altitude effect in late summer is because watersheds are dominated by high elevation meltwater which results in minimal change in $\delta^{18}O$ with elevation. Sublimation may increase $\delta^{18}O$ values (horizontal arrow). Solid circles are > 42.43° latitude (watershed centroid) while open circles are < 42.43° latitude. This threshold corresponds with the range crest where open circles are in the lee of the range. When only samples from the north (windward) side of the range are considered (excluding open circles), there is still not a significant relationship ($R^2 = 0.07$). (B) Stream water samples published by Macaulay et al. (2016) from the Issyk Kul watershed nearby (location in Fig. 3A and Supplementary Table 2), also sampled in late summer and early fall, do not show a relationship between $\delta^{18}O$ and elevation either. (C) Stream water samples published by Liu et al. (2014) across the Pamir Mountains of Tajikistan (location in Fig. 1). Solid circles are < 73.5° longitude (west) while open circles are ≥73.5° longitude (east). This boundary coincides with the threshold between late winter/spring precipitation (west) and summer precipitation (east) regimes (Fig. 2 and Supplementary Table 3) and results in a low correlation between $\delta^{18}O$ and elevation ($R^2 = 0.46$). Unlike (A) and (B), elevations for the Pamir dataset are for sample sites, not MBH. Analytical uncertainty is < ± 0.1‰ for $\delta^{18}O$.

In summary, the presence of isotopic lapse rates on the northern (windward) side of the Tian Shan in Kyrgyzstan is both temporally and spatially variable. Our data from the Shamshy transect suggest that an isotopic lapse rate does not exist for water dominated by summer precipitation and snow melt. We interpret this to be the result of seasonal precipitation partitioning, where summer precipitation falls primarily at high elevations, resulting in a watershed dominated by high elevation precipitation and snow, potentially modified slightly by evaporation and sublimation (Fig. 7A). Winter and spring $\delta^{18}O$ values along Ala Archa and San Gong transects (Fig. 6) suggest the northern flank of the Tian Shan likely exhibits seasonal isotopic lapse rates, consistent with patterns in the western Pamir (Fig. 7C) and the windward side of mountains globally (Poage and Chamberlain, 2001). We observe that an isotopic lapse rate is limited to watersheds integrating relatively significant amounts of winter and spring rainfall, which excludes the majority of high topography throughout the Tian Shan due to the seasonal change in precipitation across the range (Fig. 2).

5.4. Paleoenvironmental implications

The lack of an isotopic lapse rate on the windward side of the Tian Shan (this study) and the stark change in seasonality across the range (Fig. 2) complicate the interpretation of paleowater isotopes in this unique, continental region. Our results show that there is not a clear $\delta^{18}O$-elevation relationship for modern summer surface waters attributed to seasonal partitioning of precipitation with altitude where high elevation summer precipitation and snow melt dominate the watershed during that time. High and low elevation surface water $\delta^{18}O$ values are remarkably similar, invalidating conventional paleoaltimetry based on Rayleigh distillation for the Tian Shan. A typical isotopic lapse rate of −2.8‰/km elevation gain (Poage and Chamberlain, 2001) predicts a ~11‰ decrease across the Tian Shan (~4 km total elevation gain), notably smaller than seasonal variation observed at sites nearby which is > 15‰ (Fig. 4). Modeling by Baldwin and Vecchi (2016) suggests that Tian Shan uplift resulted in a shift from spring to summer precipitation in the mountains and lee (southeast), and increased winter and spring precipitation on the windward (northwest) side. Based on these observations, we hypothesize that paleowater $\delta^{18}O$ trends inferred from stream water proxies including fluvial carbonate cements, lacustrine carbonates, and palustrine (flood plain) paleosol carbonates are more likely to reflect changes in the seasonal distribution of precipitation than changes due to the altitude effect. Accordingly, paleoaltimetry research in the Tian Shan requires a detailed understanding of how seasonal precipitation is, and has been affected by topography through time, and how synchronous changes in both affect the isotopic composition of proxy materials.

6. Conclusions

The Tian Shan illustrate the complexity of interpreting temporal changes in the isotopic composition of meteoric water, particularly in continental environments where changes in the seasonal distribution of precipitation plays a significant role. Though data limited, transects sampled in spring show evidence of evaporation (Fig. 5) and isotopic lapse rates (Fig. 6), consistent with early spring precipitation that experienced subcloud evaporation at lower elevations. In contrast, our results show that late summer surface water in the northern Tian Shan is minimally evaporated (Fig. 5) and does not exhibit a clear isotopic lapse rate (Fig. 7A). Modern stream $\delta^{18}O$ values at high and low elevations are similar in areas influenced by summer precipitation (Fig. 7, Wang et al., 2016b), which we interpret to result from the fact that the majority of precipitation falls at relatively high elevations (> 1.5 km), dominating the hydrologic budget downstream. The segregation of seasonal precipitation with altitude and lack of a clear isotopic lapse rate during summer months challenge conventional paleoaltimetry based on Rayleigh distillation of an air mass. Accordingly, uplift of the Tian Shan may not have significantly changed meteoric water $\delta^{18}O$ values and thus may not be identifiable in regional carbonate proxy $\delta^{18}O$ records. The Tian Shan are unique in that changes in the seasonal distribution of precipitation are observed on the same spatial scale as altitudinal changes. Future work should sample streams in the middle of winter and summer to better characterize seasonal changes in river isotopic composition and extend altitudinal transects to the western flank of the Tian Shan. To better understand the source of evaporation (surface water evaporation, ice/snow sublimation, and/or subcloud evaporation), soil water and/or precipitation samples should be collected along altitudinal transects.

Appendix A. Supplementary data

Supplementary data to this article can be found online at https://doi.org/10.1016/j.chemgeo.2019.03.032.

References

Aizen, V., Aizen, E., Melack, J., Martma, T., 1996. Isotopic measurements of precipitation on central Asian glaciers (southeastern Tibet, northern Himalayas, central Tien Shan). J. Geophys. Res. 101.

Aizen, V.B., Aizen, E.M., Melack, J.M., Dozier, J., 1997. Climatic and hydrologic changes in the Tien Shan, central Asia. J. Clim. 10, 1393–1404.

Araguás-Araguás, L., Froehlich, K., Rozanski, K., 1998. Stable isotope composition of precipitation over southeast Asia. J. Geophys. Res.-Atmos. 103.

Baldwin, J., Vecchi, G., 2016. Influence of the Tian Shan on Arid Extratropical Asia. J. Clim. 29, 5741–5762.

Barry, R.G., 2012. Recent advances in mountain climate research. Theor. Appl. Climatol. 110, 549–553.

Bershaw, J., 2018. Controls on deuterium excess across Asia. Geosciences 8, 257.

Bershaw, J., Garzione, C.N., Higgins, P., MacFadden, B.J., Anaya, F., Alvarenga, H., 2010. Spatial-temporal changes in Andean plateau climate and elevation from stable isotopes of mammal teeth. Earth Planet. Sci. Lett. 289, 530–538.

Bershaw, J., Penny, S.M., Garzione, C.N., 2012. Stable isotopes of modern water across the Himalaya and eastern Tibetan Plateau: implications for estimates of paleoelevation and paleoclimate. J. Geophys. Res. Atmos. 1984–2012, 117.

Bershaw, J., J E, S., Garzione, C.N., Leier, A., Sundell, K.E., 2016. Stable isotope variations (δ18O and δD) in modern waters across the Andean Plateau. Geochim. Cosmochim. Acta 194, 310–324.

Blumer, F.P., 1998. Investigations of the precipitation conditions in the central part of the Tianshan mountains. Hydrology 248, 343–350.

Böhner, J., 2006. General climatic controls and topoclimatic variations in Central and High Asia. Boreas 35, 279–295.

Bony, S., Risi, C., Vimeux, F., 2008. Influence of convective processes on the isotopic composition (d18O and dD) of precipitation and water vapor in the tropics: 1. Radiative-convective equilibrium and Tropical ocean–Global Atmosphere–Coupled Ocean-Atmosphere Response Experiment (TOGA-COARE) simulations. J. Geophys. Res. Atmos. 113, D19305.

Bothe, O., Fraedrich, K., Zhu, X., 2011. Precipitation climate of Central Asia and the large-scale atmospheric circulation. Theor. Appl. Climatol. 108, 345–354.

Breecker, D.O., Sharp, Z.D., McFadden, L.D., 2009. Seasonal bias in the formation and stable isotopic composition of pedogenic carbonate in modern soils from central New Mexico, USA. Geol. Soc. Am. Bull. 121, 630–640.

Caves, J.K., Bayshashov, B.U., Zhamangara, A., Ritch, A.J., Ibarra, D.E., Sjostrom, D.J., Mix, H.T., Winnick, M.J., Chamberlain, C.P., 2017. Late miocene uplift of the Tian Shan and Altai and reorganization of central Asia climate. GSA Today 27, 20–26.

Cerling, T.E., Quade, J., 1993. Stable carbon and oxygen isotopes in soil carbonates. In: Climate Change in Continental Isotopic Records, vol. 78. pp. 217–231.

Chamberlain, C., Poage, M., 2000. Reconstructing the paleotopography of mountain belts from the isotopic composition of authigenic minerals. Geology 28, 115.

Chang, D.H., 1983. The Tibetan Plateau in relation to the vegetation of China. Ann. Mo. Bot. Gard. 564–570.

Charreau, J., Kent-Corson, M.L., Barrier, L., Augier, R., Ritts, B.D., Chen, Y., France-Lannord, C., Guilmette, C., 2012. A high-resolution stable isotopic record from the Junggar Basin (NW China): implications for the paleotopographic evolution of the Tianshan Mountains. Earth Planet. Sci. Lett. 341, 158–169.

Craig, H., 1961. Isotopic variations in meteoric waters. Science 133, 1702–1703.

Cui, J., An, S., Wang, Z., Fang, C., Liu, Y., Yang, H., Xu, Z., Liu, S., 2009. Using deuterium excess to determine the sources of high-altitude precipitation: implications in hydrological relations between sub-alpine forests and alpine meadows. J. Hydrol. 373, 24–33.

Dumitru, T.A., Zhou, D., Chang, E.Z., Graham, S.A., Hendrix, M.S., Sobel, E.R., Carroll, A.R., 2001. Uplift, exhumation, and deformation in the Chinese Tian Shan. Mem. Geol. Soc. Am. 71–100.

Fan, Y., Chen, Y., Li, X., Li, W., Li, Q., 2015. Characteristics of water isotopes and ice-snowmelt quantification in the Tizinafu River, north Kunlun Mountains, Central Asia. Quat. Int. 380, 116–122.

Friedman, I., Gleason, J., Warden, A., 1993. Ancient climate from deuterium content of water in volcanic glass. In: Climate Change in Continental Isotopic Recordspp. 309–319.

Froehlich, K., Kralik, M., Papesch, W., Rank, D., Scheifinger, H., Stichler, W., 2008. Deuterium excess in precipitation of Alpine regions–moisture recycling. Isot. Environ.

Health Stud. 44, 61–70.
Garzione, C.N., Dettman, D.L.Q.J., DeCelles, P.G.B.R.F., 2000. High times on the Tibetan Plateau; paleoelevation of the Thakkhola Graben, Nepal. Geology 28, 339–342.
Gat, J., 1996. Oxygen and hydrogen isotopes in the hydrologic cycle. Annu. Rev. Earth Planet. Sci. 24, 225–262.
Gat, J.R., Airey, P.L., 2006. Stable water isotopes in the atmosphere/biosphere/lithosphere interface: scaling-up from the local to continental scale, under humid and dry conditions. Glob. Planet. Chang. 51, 25–33.
Gat, J., Carmi, I., 1970. Evolution of the isotopic composition of atmospheric waters in the Mediterranean Sea area. J. Geophys. Res. 75, 3039–3048.
Gile, L.H., Peterson, F.F., Grossman, R.B., 1966. Morphological and genetic sequences of carbonate accumulation in desert soils. Soil Sci. 101, 347–360.
Gonfiantini, R., Roche, M.-A., Olivry, J.-C., Fontes, J.-C., Zuppi, G.M., 2001. The altitude effect on the isotopic composition of tropical rains. Chem. Geol. 181, 147–167.
Graham, S.A., Chamberlain, C.P., Yue, Y., Ritts, B.D., Hanson, A.D., Horton, T.W., Waldbauer, J.R., Poage, M.A., Feng, X., 2005. Stable isotope records of Cenozoic climate and topography, Tibetan plateau and Tarim basin. Am. J. Sci. 305, 101–118.
Guan, H., Zhang, X., Skrzypek, G., Sun, Z., Xu, X., 2013. Deuterium excess variations of rainfall events in a coastal area of South Australia and its relationship with synoptic weather systems and atmospheric moisture sources. J. Geophys. Res. Atmos. 118, 1123–1138.
Gupta, S., Deshpande, R., Bhattacharya, S., Jani, R., 2005. Groundwater δ 18 O and δD from central Indian Peninsula: influence of the Arabian Sea and the Bay of Bengal branches of the summer monsoon. J. Hydrol. 303, 38–55.
Haiyan, C., Yaning, C., Weihong, L., Xinming, H., Yupeng, L., Qifei, Z., 2018. Identifying evaporation fractionation and streamflow components based on stable isotopes in the Kaidu River Basin with mountain-oasis system in northwest China. Hydrol. Process. 32, 2423–2434.
Hren, M.T., Bookhagen, B., Blisniuk, P.M., Booth, A.L., Chamberlain, C.P., 2009. δ 18 O and δD of streamwaters across the Himalaya and Tibetan Plateau: implications for moisture sources and paleoelevation reconstructions. Earth Planet. Sci. Lett. 288, 20–32.
Huang, T., Pang, Z., 2010. Changes in groundwater induced by water diversion in the Lower Tarim River, Xinjiang Uygur, NW China: evidence from environmental isotopes and water chemistry. J. Hydrol. 387, 188–201.
IAEA/WMO, 2018. Global Network of Isotopes in Precipitation, the GNIP Database. Accessible at. http://isohis.iaea.org.
Jouzel, J., Merlivat, L., 1984. Deuterium and oxygen 18 in precipitation: modeling of the isotopic effects during snow formation. J. Geophys. Res. Atmos. 89, 11749–11757 (1984–2012).
Kar, N., Garzione, C.N., Jaramillo, C., Shanahan, T., Carlotto, V., Pullen, A., Moreno, F., Anderson, V., Moreno, E., Eiler, J., 2016. Rapid regional surface uplift of the northern Altiplano plateau revealed by multiproxy paleoclimate reconstruction. Earth Planet. Sci. Lett. 447, 33–47.
Karim, A., Veizer, J., 2002. Water balance of the Indus River Basin and moisture source in the Karakoram and western Himalayas: implications from hydrogen and oxygen isotopes in river water. J. Geophys. Res. Atmos. 107.
Kendall, C., Coplen, T.B., 2001. Distribution of oxygen-18 and deuterium in river waters across the United States. Hydrol. Process. 15, 1363–1393.
Kent-Corson, M.L., Ritts, B.D., Zhuang, G., Bovet, P.M., Graham, S.A., Page Chamberlain, C., 2009. Stable isotopic constraints on the tectonic, topographic, and climatic evolution of the northern margin of the Tibetan Plateau. Earth Planet. Sci. Lett. 282, 158–166.
Klinge, M., Böhner, J., Erasmi, S., 2015. Modeling forest lines and forest distribution patterns with remote-sensing data in a mountainous region of semiarid central Asia. Biogeosciences 12, 2893–2905.
Kohn, M.J., Cerling, T.E., 2002. Stable isotope compositions of biological apatite. In: Phosphates; Geochemical, Geobiological, and Materials Importance, vol. 48. pp. 455–488.
Kong, Y., Pang, Z., Froehlich, K., 2013. Quantifying recycled moisture fraction in precipitation of an arid region using deuterium excess. Tellus B 65.
Kreutz, K.J., Wake, C.P., Aizen, V.B., Cecil, L.D., Synal, H.-A., 2003. Seasonal deuterium excess in a Tien Shan ice core: influence of moisture transport and recycling in Central Asia. Geophys. Res. Lett. 30.
Kurita, N., Yamada, H., 2008. The role of local moisture recycling evaluated using stable isotope data from over the middle of the Tibetan Plateau during the monsoon season. J. Hydrometeorol. 9, 760–775.
Lechler, A.R., Niemi, N.A., 2011a. Controls on the spatial variability of modern meteoric δ18O: empirical constraints from the western US and East Asia and implications for stable isotope studies. Am. J. Sci. 311, 664–700.
Lechler, A.R., Niemi, N.A., 2011b. The influence of snow sublimation on the isotopic composition of spring and surface waters in the southwestern United States: implications for stable isotope–based paleoaltimetry and hydrologic studies. Geol. Soc. Am. Bull. B30467, 30461.
Lee, J.E., Fung, I., 2008. "Amount effect" of water isotopes and quantitative analysis of post-condensation processes. Hydrol. Process. 22, 1–8.
Leier, A., McQuarrie, N., Garzione, C., Eiler, J., 2013. Stable isotope evidence for multiple pulses of rapid surface uplift in the Central Andes, Bolivia. Earth Planet. Sci. Lett. 371, 49–58.
Li, L., Garzione, C.N., 2017. Spatial distribution and controlling factors of stable isotopes in meteoric waters on the Tibetan Plateau: implications for paleoelevation reconstruction. Earth Planet. Sci. Lett. 460, 302–314.
Liotta, M., Favara, R., Valenza, M., 2006. Isotopic composition of the precipitations in the central Mediterranean: origin marks and orographic precipitation effects. J. Geophys. Res. Atmos. 1984–2012, 111.
Liu, Q., Tian, L.D., Wang, J.L., Wen, R., Weng, Y.B., Shen, Y.P., Vladislav, M., Kanaev, E., 2014. A study of longitudinal and altitudinal variations in surface water stable isotopes in West Pamir, Tajikistan. Atmos. Res. 153, 10–18.
Liu, X., Rao, Z., Zhang, X., Huang, W., Chen, J., Chen, F., 2015. Variations in the oxygen isotopic composition of precipitation in the Tianshan Mountains region and their significance for the Westerly circulation. J. Geogr. Sci. 25, 801–816.
Lu, B., Sun, T., Wang, C., Dai, S., Kuang, J., Wang, J., 2012. Temporal and spatial variations of δ 18 O along the main stem of Yangtze River, China. In: Monitoring Isotopes in Rivers: Creation of the Global Network of Isotopes in Rivers (GNIR). Vienna, pp. 211–220.
Macaulay, E.A., Sobel, E.R., Mikolaichuk, A., Wack, M., Gilder, S.A., Mulch, A., Fortuna, A.B., Hynek, S., Apayarov, F., 2016. The sedimentary record of the Issyk Kul basin, Kyrgyzstan: climatic and tectonic inferences. Basin Res. 28, 57–80.
Morris, B.L., George Darling, W., Gooddy, D.C., Litvak, R.G., Neumann, I., Nemaltseva, E.J., Poddubnaia, I., 2005. Assessing the extent of induced leakage to an urban aquifer using environmental tracers: an example from Bishkek, capital of Kyrgyzstan, Central Asia. Hydrogeol. J. 14, 225–243.
Mulch, A., Graham, S.A., Chamberlain, C.P., 2006. Hydrogen isotopes in Eocene river gravels and paleoelevation of the Sierra Nevada. Science 313, 87–89.
Numaguti, A., 1999. Origin and recycling processes of precipitating water over the Eurasian continent: experiments using an atmospheric general circulation model. J. Geophys. Res. 104, 1957–1972.
Poage, M.A., Chamberlain, C.P., 2001. Empirical relationships between elevation and the stable isotope composition of precipitation and surface waters; considerations for studies of paleoelevation change. Am. J. Sci. 301, 1–15.
Rank, D., Papesch, W., 2005. Isotopic composition of precipitation in Austria in relation to air circulation patterns and climate. In: Isotopic Composition of Precipitation in the Mediterranean Basin in Relation to Air Circulation Patterns and Climate, IAEA-TECDOC-1453, IAEA, Vienna, pp. 19–36.
Risi, C., Bony, S., Vimeux, F., 2008. Influence of convective processes on the isotopic composition (d18O and dD) of precipitation and water vapor in the tropics: 2. Physical interpretation of the amount effect. J. Geophys. Res. Atmos. 113, D19306.
Rohrmann, A., Strecker, M.R., Bookhagen, B., Mulch, A., Sachse, D., Pingel, H., Alonso, R.N., Schildgen, T.F., Montero, C., 2014. Can stable isotopes ride out the storms? The role of convection for water isotopes in models, records, and paleoaltimetry studies in the central Andes. Earth Planet. Sci. Lett. 407, 187–195.
Rowley, D.B., Garzione, C.N., 2007. Stable isotope-based paleoaltimetry. Annu. Rev. Earth Planet. Sci. 35, 463–508.
Rozanski, K., Araguas-Araguas, L., Gonfiantini, R., 1993. Isotopic patterns in modern global precipitation. In: Climate Change in Continental Isotopic Records, vol. 78. pp. 1–36.
Sachse, D., Billault, I., Bowen, G.J., Chikaraishi, Y., Dawson, T.E., Feakins, S.J., Freeman, K.H., Magill, C.R., McInerney, F.A., Van der Meer, M.T., 2012. Molecular paleohydrology: interpreting the hydrogen-isotopic composition of lipid biomarkers from photosynthesizing organisms. Annu. Rev. Earth Planet. Sci. 40.
Savin, S.M., Hsieh, J.C., 1998. The hydrogen and oxygen isotope geochemistry of pedogenic clay minerals: principles and theoretical background. Geoderma 82, 227–253.
Saylor, J.E., Horton, B.K., 2014. Nonuniform surface uplift of the Andean plateau revealed by deuterium isotopes in Miocene volcanic glass from southern Peru. Earth Planet. Sci. Lett. 387, 120–131.
Schiemann, R., Lüthi, D., Schär, C., 2009. Seasonality and interannual variability of the westerly jet in the Tibetan Plateau region. J. Clim. 22, 2940–2957.
Shi, Y., Shen, Y., Kang, E., Li, D., Ding, Y., Zhang, G., Hu, R., 2007. Recent and future climate change in northwest China. Clim. Chang. 80, 379–393.
Talbot, M., 1990. A review of the palaeohydrological interpretation of carbon and oxygen isotopic ratios in primary lacustrine carbonates. Chem. Geol. Isot. Geosci. 80, 261–279.
Tian, L., Masson-Delmotte, V., Stievenard, M., Yao, T., Jouzel, J., 2001. Tibetan Plateau summer monsoon northward extent revealed by measurements of water stable isotopes. J. Geophys. Res. 106, 28081–28088.
Tian, L., Yao, T., White, J., Yu, W., Wang, N., 2005. Westerly moisture transport to the middle of Himalayas revealed from the high deuterium excess. Chin. Sci. Bull. 50, 1026–1030.
Tian, L., Yao, T., MacClune, K., White, J.W.C., Schilla, A., Vaughn, B., Vachon, R., Ichiyanagi, K., 2007. Stable isotopic variations in west China: a consideration of moisture sources. J. Geophys. Res. Atmos. 112, 10112.
Wang, Y., Cheng, H., Edwards, R.L., Kong, X., Shao, X., Chen, S., Wu, J., Jiang, X., Wang, X., An, Z., 2008. Millennial-and orbital-scale changes in the East Asian monsoon over the past 224,000 years. Nature 451, 1090–1093.
Wang, S., Zhang, M., Che, Y., Zhu, X., Liu, X., 2016a. Influence of below-cloud evaporation on deuterium excess in precipitation of arid central Asia and its meteorological controls. J. Hydrometeorol. 17, 1973–1984.
Wang, S., Zhang, M., Hughes, C.E., Zhu, X., Dong, L., Ren, Z., Chen, F., 2016b. Factors controlling stable isotope composition of precipitation in arid conditions: an observation network in the Tianshan Mountains, central Asia. Tellus B 68.
World Bank, 2018. Climate Change Knowledge Portal, Historical Data. Accessible at. http://sdwebx.worldbank.org/.
Yao, T., Masson-Delmotte, V., Gao, J., Yu, W., Yang, X., Risi, C., Sturm, C., Werner, M., Zhao, H., He, Y., 2013. A review of climatic controls on δ18O in precipitation over the Tibetan Plateau: observations and simulations. Rev. Geophys. 51, 525–548.
Yatagai, A., Yasunari, T., 1998. Variation of summer water vapor transport related to precipitation over and around the arid region in the interior of the Eurasian continent. J. Meteorol. Soc. Jpn. 2 (76), 799–815.
Yu, Y., Wang, J., Li, Q., 2003. Spatial and temporal distribution of water vapor and its variation trend in atmosphere over Northwest China. J. Glaciol. Geocryol. 25, 149–156.